Revista Mexicana de Astronomía y Astrofísica, **36**, 161–169 (2000)

A NEW WARM MOLECULAR CLUMP TOWARD THE STAR FORMING REGION G34.26+0.15

Y. Gómez, C. A. Rodríguez-Rico, and L. F. Rodríguez

Instituto de Astronomía, UNAM, Morelia

and

G. Garay

Departamento de Astronomía, Universidad de Chile

Received 2000 August 21; accepted 2000 September 13

RESUMEN

Se reanalizaron observaciones de amoníaco hechas con el VLA hacia la región de formación estelar G34.26+0.15. Se encontró un nuevo grumo de gas molecular hacia el noroeste con emisión (2,2) y (3,3) de amoníaco, además de la estructura molecular previamente conocida. El nuevo grumo está asociado con máseres de agua y se le estimó una temperatura rotacional de $\sim 54 \pm 12$ K, un diámetro de ~ 0.15 pc (suponiendo una distancia de 3.8 kpc) y una masa molecular de $\sim 10\ M_\odot$ (suponiendo un cociente $[H_2/NH_3]$ de 10^7). Estos resultados sugieren que el grumo podría tener una estrella embebida y que además de las estrellas masivas que excitan las regiones H II previamente reportadas, pueden existir otras estrellas jóvenes de menor masa en la región.

ABSTRACT

In this work we reanalyze VLA ammonia (2,2) and (3,3) observations toward the massive star forming region G34.26+0.15. We find one new ammonia clump with (2,2) and (3,3) emission toward the northwest in addition to the main molecular structure previously reported. The new clump is associated with water maser spots and we estimate for it a rotational temperature of $\sim 54 \pm 12$ K, a diameter of 0.15 pc (assuming a distance of 3.8 kpc) and a molecular mass of $\sim 10\ M_\odot$ (assuming an $[H_2/NH_3]$ ratio of 10^7). These results suggest that the clump could have an embedded star and that in addition to the massive stars that excite the H II regions previously reported, there may be other young stars of lower mass in the region.

Key Words: **H II REGIONS — ISM: MOLECULES — RADIO LINES: ISM — STARS: FORMATION**

1. INTRODUCTION

Ultracompact H II regions are small (< 0.1 pc) and dense ($n_e > 10^4$ cm^{-3}) regions of ionized gas generally excited by O and B stars that are still embedded in their natal molecular cloud (Ryle & Downes 1967; Wood & Churchwell 1989). The presence of maser emission and warm molecular gas are strong indicators of recent star formation (cf. Garay & Lizano 1999 and references therein). G34.26+0.15 has been extensively studied in radio continuum (Turner et al 1974; Reid & Ho 1985; Wood & Churchwell 1989), radio recombination lines (Garay, Reid, & Moran 1985; Garay, Rodríguez, & van Gorkom 1986; Gaume, Fey, & Claussen 1994; Fey et al. 1994) and molecular lines (Benson & Johnston 1984; Heaton et al. 1985; Andersson & Garay 1986; Gaume & Mutel 1987; Keto, Ho, & Reid 1987; Garay & Rodríguez 1990; Carral & Welch 1992). At radio continuum frequencies it exhibits several components: an ultracompact H II region with a cometary shape named component C (Reid & Ho 1985; Garay et al. 1986; Wood & Churchwell 1989; Gaume et al. 1994), two ultracompact H II regions called A and B with diameter less than 2000 AU (Reid & Ho 1985; Garay & Rodríguez 1990), and an extended ring-like H II region with a diameter of 1′ called component D

(Reid & Ho 1985; Fey et al. 1992; Fey et al. 1994). H_2O and OH maser emission have been observed toward G34.26+0.15 (Genzel & Downes 1977; Garay et al. 1985; Gaume & Mutel 1987; Fey et al. 1994). Molecular gas has been mapped in NH_3, HCO^+, SO, CH_3CN, and CO (Heaton, Little, & Bishop 1989; Andersson & Garay 1986; Carral, Welch, & Wright 1987; Henkel, Wilson, & Mauersberger 1987; Carral & Welch 1992; Garay & Rodríguez 1990; Churchwell, Walmsley, & Wood 1992; Heaton et al. 1993: Akeson & Carlstrom 1996; Watt & Mundy 1999) showing the presence of a molecular structure located close to the "head" of the cometary H II region. The kinematics of the molecular gas shows a velocity gradient of $\sim$ 15 km s^{-1} pc^{-1} in $\sim$ 0.2 pc (Carral & Welch 1992; Akeson & Carlstrom 1996; this paper) which is in opposite sense to the velocity gradient of the ionized gas across component C observed in radio recombination lines (Garay et al. 1986; Gaume et al. 1994).

Garay & Rodríguez (1990) interpreted the ammonia emission as arising from two main components of molecular material: a warm, optically thick disk-like clump (T $\sim$ 60 K, $n_{H_2} \sim 10^6$ cm^{-3}) and a molecular envelope around it (T $\sim$ 18 K, $n_{H_2} \sim 10^4$ cm^{-3}).

In this work we reanalyzed the VLA data of the (2,2) and (3,3) inversion transitions of ammonia taken from Garay & Rodríguez (1990) in order to search for emission toward the recently identified millimeter source G34.24+0.13MM, located 84″ southeast of component C, that has been interpreted as a deeply embedded proto-B star (Hunter et al. 1998). No ammonia emission was detected at a 3-sigma level of 30 mJy $beam^{-1}$ toward the millimeter source, but we found one new ammonia clump toward the northwest of G34.26+0.15 which is closely associated with water maser spots.

2. OBSERVATIONS

The observations were made using the Very Large Array (VLA) of the NRAO[1]. All data were edited and calibrated following standard procedures and maps were made using the NRAO software AIPS. The observations were taken on January 23, 1986 in the D configuration toward the star forming region G34.26+0.15. A summary of the observations is reported in Garay & Rodríguez (1990). The (J,K) = (2,2) and (3,3) inversion transitions of the ammonia molecule (NH_3) were observed assuming a rest frequency of 23722.633 and 23870.129 MHz, respectively. The bandpass was 12.5 MHz, centered at an LSR velocity of 55 km s^{-1}, and we used 31 spectral channels 195.3 KHz wide each ($\sim$ 2.5 km s^{-1} at the observing frequencies). The flux density scale was determined from observations of the amplitude calibrator 3C 286, for which a flux density of 2.93 Jy was assumed. The phase calibrator was 1749+096, for which a bootstrapped 1.3 cm flux density of 3.70 $\pm$ 0.09 Jy was obtained. The shape of the bandpass was determined from observations of the source 3C 84, from which we determine a flux density of 34 $\pm$ 2 Jy. Line data were self-calibrated (Schwab 1980) in phase and amplitude using the continuum channel (including the central 75% of the bandpass). The continuum (line-free) channels were subtracted from the visibility data by use of the task UVLIN. Maps were made by using the task IMAGR with the robust parameter of Briggs (1995) set equal to 5 (equivalent to natural weight) and a Gaussian taper of 30 kλ which resulted in a synthesized beam of $\sim$ 7″$\times$ 6″ for the (2,2) and (3,3) transitions. The rms noise level in a single spectral line channel were about 11 and 13 mJy $beam^{-1}$ for the (2,2) and (3,3) observations, respectively.

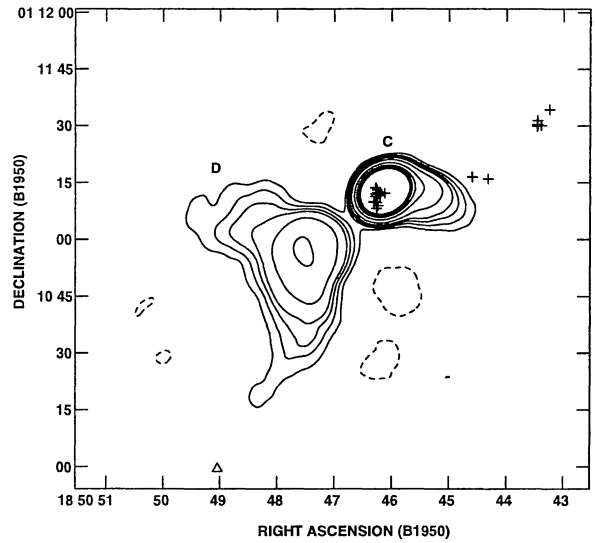

Fig. 1. VLA continuum contour map of G34.3+0.15 at 1.3 cm with $\sim$ 7″ resolution. Contour levels are −3, 3, 5, 7, 9, 15, 30, 50, 70, and 90 times 6 mJy/beam, the rms noise of the map. The crosses indicate the position of the H_2O masers reported by Fey et al. 1994. The small triangle at the bottom of the figure marks the position of the millimeter source proposed as a massive protostellar object (Hunter et al. 1998)

[1]The National Radio Astronomy Observatory is operated by Associated Universities, Inc., under cooperative agreement with the National Science Foundation.

TABLE 1

OBSERVED RADIO CONTINUUM PARAMETERS AT 1.3 CM

Component	Flux Density (Jy)	Peak Flux (mJy/beam)	α (1950) (h m s)	δ (1950) (° ′ ″)	Deconv. Size (″)
C	5.1 ± 0.1[a]	4200	18 50 46.14	01 11 12.7	∼ 3
D	1.6 ± 0.1	194	18 50 47.55	01 10 57.0	∼ 20

[a] Includes flux density of compact components A and B.

3. RESULTS AND DISCUSSION

3.1. *Continuum*

Figure 1 shows a 1.3 cm radio continuum self-calibrated map made from the continuum channel of the (2,2) data. The map exhibits the bright cometary-like H II region (component C) and the extended ring-like H II region to the southeast (component D). The observed radio continuum parameters of these components are show in Table 1. Note that the A and B compact H II regions are not resolved and they appear blended with component C due to the low angular resolution of the observations (∼ 7″). For component C we estimate a luminosity of 2.5 × 10^5 $L_\odot$, which is equivalent to that provided by an O6 ZAMS star, in good agreement with previous estimates (Andersson & Garay 1986; Garay et al. 1986; Heaton et al. 1989; Garay & Rodríguez 1990).

3.2. *Molecular Gas*

Line maps in the (2,2) and (3,3) transitions of ammonia, shown in Figure 2, reveal the presence of an extended molecular structure toward component C (0.2 × 0.1 pc), which is seen in the velocity range from 52.5 km s^{-1} to 64.9 km s^{-1} and centered at ∼ 59 km s^{-1}. Figure 3 presents contours of the velocity integrated (2,2) line emission (from 52.5 to 64.8 km s^{-1}) overlaid on a 1.3 cm continuum contour which indicates the extent of the ratio continuum tracing the free-free emission. Based on the morphology, it is possible to identify five different ammonia components, including the new ammonia clump (component 4) reported here. The spectra of the spatially integrated (2,2) and (3,3) ammonia emission from the four clearly detected (see below) ammonia components (marked with boxes in Fig. 3) are presented in Figure 4. The parameters of the main ammonia lines from each component, determined by fitting a Gaussian profile to the corresponding spectra, are given in Table 2. Component 1 shows the main (2,2) transition of ammonia in absorption and the main (3,3) line in emission, a situation that was interpreted by Garay & Rodríguez (1990) as due to a blend, within a synthesized beam, of two components of molecular gas in front of the H II region: a warm, optically thick cloud of gas very close to the H II region, and an extended component of cold gas with moderate optical depth. Components 2 and 3 exhibit the main (2,2) and (3,3) ammonia lines in emission. The presence of component 3 was not reported by Garay & Rodríguez (1990) but it appears detected in the (3,3) ammonia transition map by Heaton et al. (1989). Components 4 and 5 are weak, new ammonia clumps that are associated with water masers. Since component 5 is only marginally detected (∼ 4 σ level) in the (2,2) ammonia transition and not detected in the main (3,3) ammonia line, we will not consider it further. However, we note that emission at 350 μm (Hunter et al. 1998) and HCO^+ (Carral & Welch 1992) has been detected at position of component 5. More sensitive observations are needed to confirm this ammonia clump. Component 4 has been considered in this work as a new molecular clump because it was detected in both (2,2) and (3,3) ammonia lines, and it is associated with water maser emission. Until now no radio continuum has been found toward this position. Garay et al. (1986) set a 5-σ level of 0.5 mJy $beam^{-1}$ at 14.7 GHz.

3.3. *The New Ammonia Clump in G34.26+0.15: Component 4*

The average central velocity of the molecular gas in emission in components 1, 2, and 3 is around 59 km s^{-1}, whereas the average velocity of component 4 is aproximately 61 km s^{-1}, which is slightly redshifted with respect to the other components. This new ammonia clump has four water masers associated with it (Fey et al. 1994), as can be seen in Fig. 3. Three of these masers are located just at the center of the clump and have an average velocity of ∼ −15 km s^{-1}, the other water maser spot, which is at the edge of the clump, has a velocity of +36.3 km s^{-1}. All these masers appear blueshifted with re-

TABLE 2

AMMONIA LINE PARAMETERS

Component	Transition	Flux Density (mJy)	V_{LSR} (km s^{-1})	ΔV (km s^{-1})
1	(2,2;m)	-200 ± 47	62.4 ± 0.6	4.2 ± 1.0
	(3,3;m)	266 ± 32	59.3 ± 0.5	8.5 ± 1.0
2	(2,2;m)	251 ± 40	57.2 ± 0.5	6.9 ± 1.3
	(3,3;m)	469 ± 35	59.3 ± 0.3	9.6 ± 0.8
3	(2,2;m)	156 ± 20	58.2 ± 0.4	6.4 ± 1.0
	(3,3;m)	245 ± 20	59.7 ± 0.2	6.1 ± 0.6
4	(2,2;m)	41 ± 6	60.8 ± 0.5	7.9 ± 1.3
	(3,3;m)	56 ± 6	61.2 ± 0.3	6.8 ± 0.8

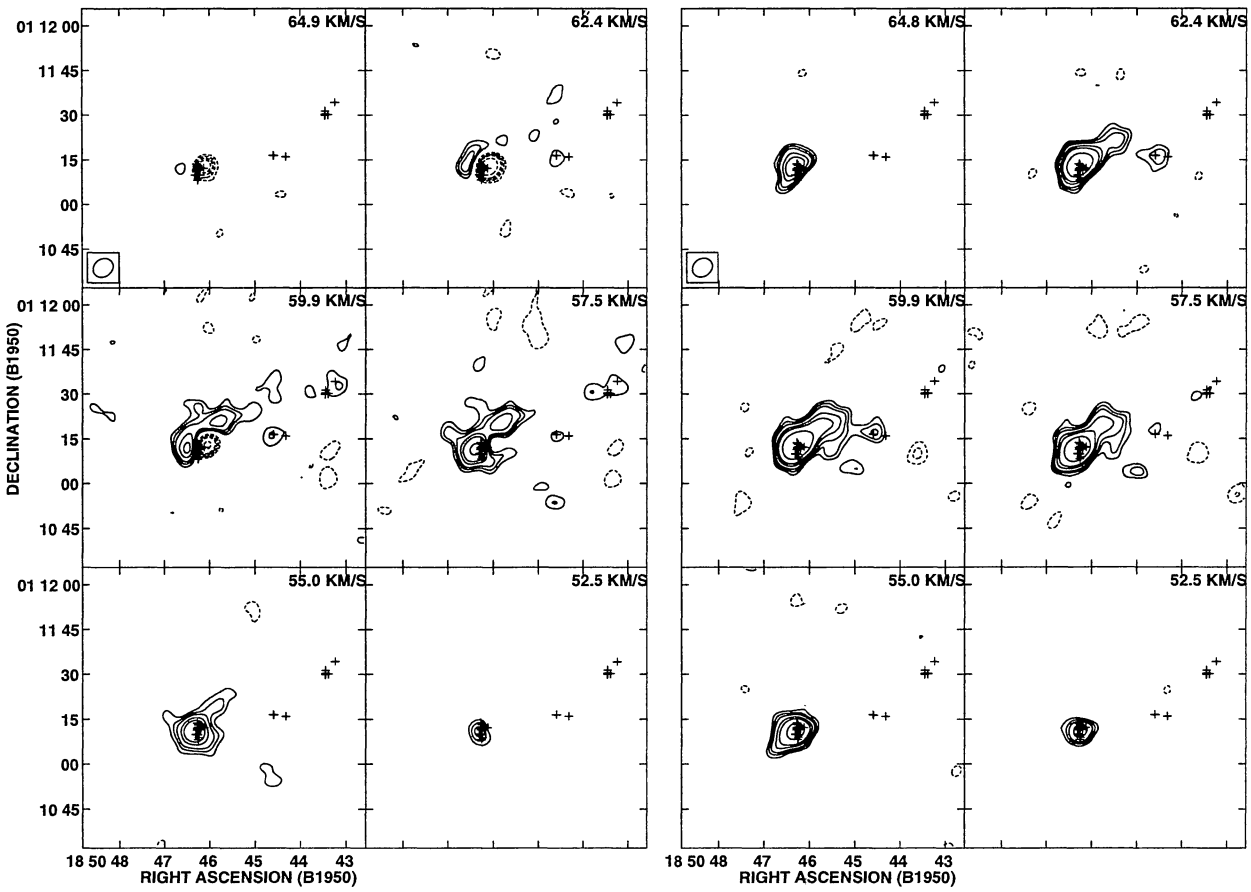

Fig. 2. Channel maps of the ammonia (2,2) and (3,3) transitions toward the G34.26+0.15 region. Left: (2,2) transition. Contour levels are −15, −9, −7, −5, −3, 3, 4, 5, 7, 9, and 15 × 11 mJy beam^{-1}, the rms noise of the maps. Right: (3,3) transition. Contour levels are −3, 3, 4, 5, 7, 9, and 15 × 13 mJy beam^{-1}, the rms noise of the maps.

spect to the ammonia gas velocity (∼ +61 km s^{-1}). Given the coincidence in position between the ammonia gas and the water masers we consider that the masers are associated with the clump. The large velocity difference between the ammonia and the water masers suggests that there may be outflow activity

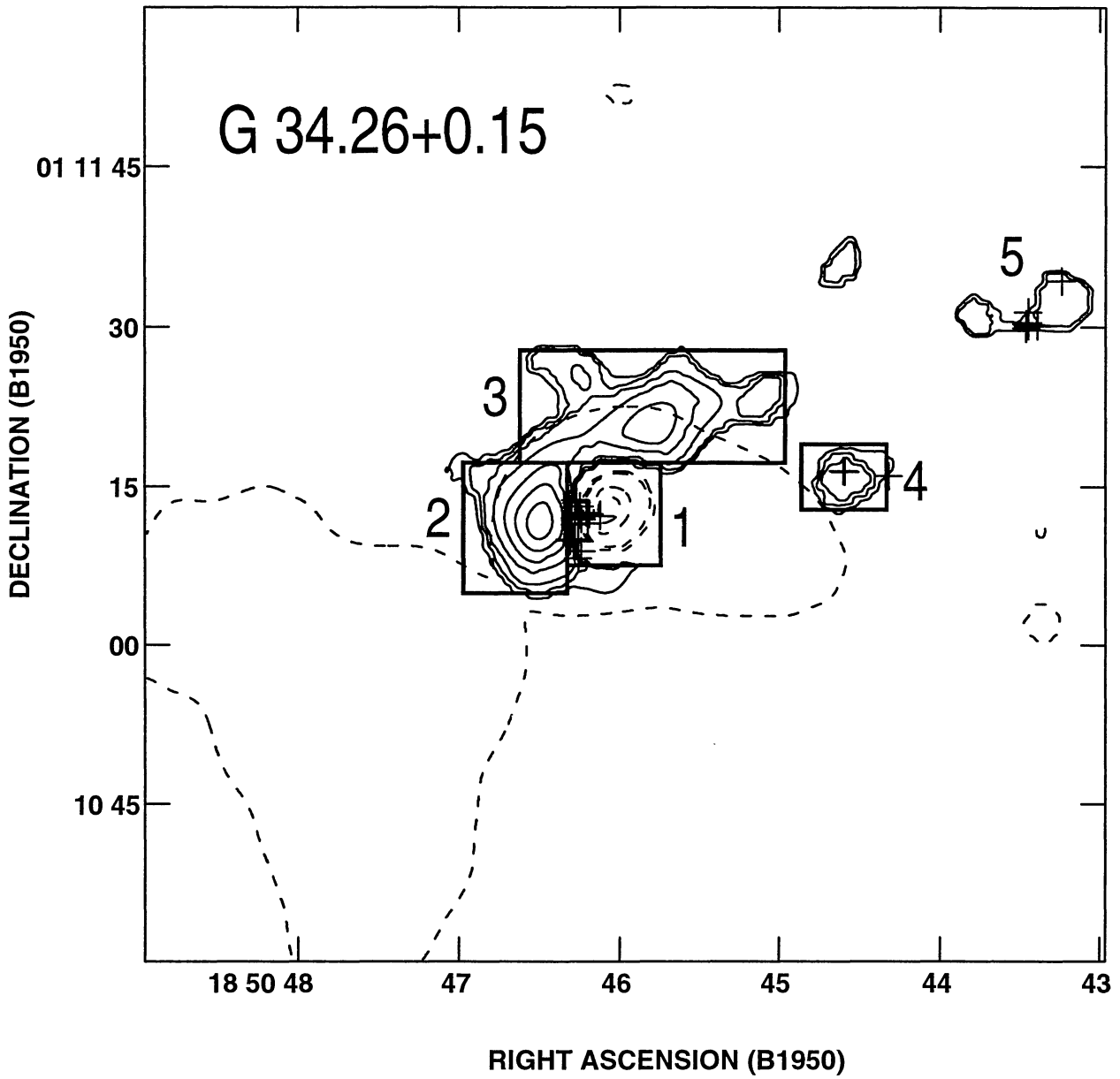

Fig. 3. Contour map of the zero moment of the (2,2) emission toward the H II complex. The extent of the 1.3 cm radio continuum emission is shown with a dashed line. Contour levels are −90, −70, −50, −30, −20, 10, 15, 20, 30, 40, 50, 60, 70, 80, and 90 percent of 120 mJy beam^{-1} km s^{-1}. The different ammonia components, including the new ammonia clump, are enclosed in thick-line rectangles and indicated with numbers. The crosses indicate the position of the H_2O maser spots (Fey et al. 1994).

associated with this clump.

Since both the (2,2) and (3,3) main lines appear in emission toward component 4 (see Fig. 2), this allows us to estimate the rotational temperature of the ammonia clump. Assuming an LTE ortho-para ratio for the NH_3 molecule and assuming that the emission is optically thin, the average rotational temperature from the ratio of the (2,2) and (3,3) main lines is given by

$$T_{rot}(33,22) = 59.6\left[ln\left(3.5\frac{S_L(2,2)\Delta v(2,2)}{S_L(3,3)\Delta v(3,3)}\right)\right]^{-1} K,$$

where $S_L(J,K)$ and $\Delta v(J,K)$ are the flux density and the line width of the main line of the (J,K) inver-

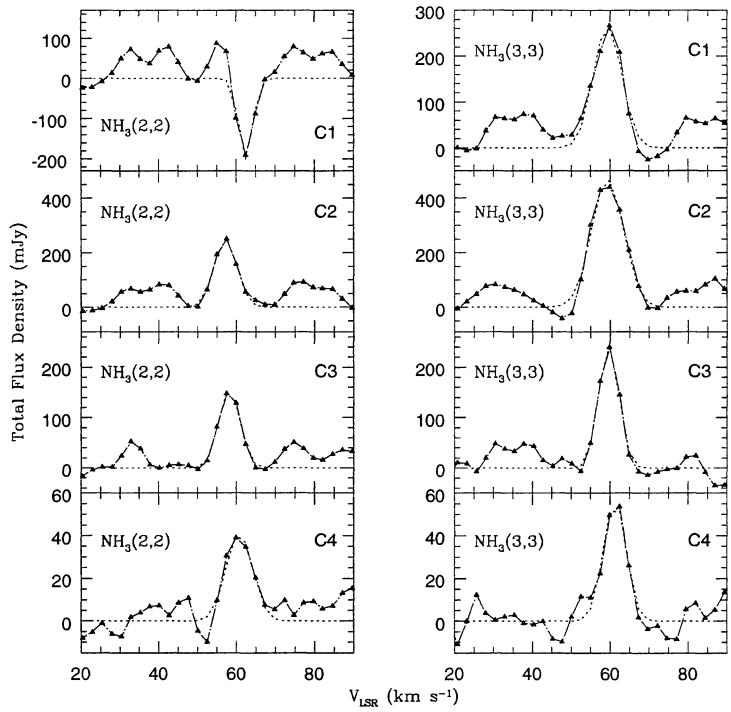

Fig. 4. Spectra of the spatially integrated (2,2) and (3,3) ammonia emission from four different components (marked with boxes in Figure 3) identified toward G34.26+0.15. The fit to the main transition is shown with dashed lines.

sion transition. Using the parameters given in Table 2 for this component we derive an average rotational temperature of $\sim$ 54 $\pm$ 12 K. This warm temperature suggests the presence of an embedded star. A B0 ZAMS embedded star (with luminosity of $\sim 2.5 \times 10^4\ L_\odot$) could provide the observed temperature. One difficulty with this interpretation is that, if an optically-thin H II region is produced by the B0 ZAMS star, a source with flux density of order $\sim 10^2$ mJy would be expected. This flux density is well above the upper limit of $\sim$0.5 mJy (Garay et al. 1986). However, it is well known that observed flux densities from H II regions excited by young massive stars are much lower than expected (Carral et al. 1999).

Can the heating be provided externally by the O6 ZAMS star ($\sim 2.5 \times 10^5\ L_\odot$) that ionizes the cometary H II region (component C)? We assume a distance from the H II region to the clump of $\sim$ 0.55 pc (30″ at a distance of 3.8 kpc). Following Scoville & Kwan (1976) and assuming that there is no absorption between the O6 star and the ammonia clump and a dust absorptivity frequency dependence of ν^{+1}, we derive a temperature of $\sim$ 50 K, similar to the derived rotational temperature. In this case, the clump could be heated externally by the central star of the H II region. However, most likely there is considerable opacity between the two objects and following the discussion of Scoville & Kwan (1976) and Natta et al. (1981) a lower value, of order 25 K, would be expected for the temperature of the clump, if externally heated.

Given the uncertainties in our knowledge of the conditions in this complex region, we cannot argue in a compelling way for the presence of a star embedded in the clump. However, the association with water masers and the warm temperature of the clump suggest an embedded energy source.

Assuming an LTE population for all ammonia levels, it is possible to estimate the total column density of NH_3 for the clump knowing the optical depth of a (J,K) inversion transition and the rotational temperature, by the relation (Garay & Rodríguez 1990)

$$N(NH_3) = \frac{1.65 \times 10^{14}\ J(J+1)}{\nu\ g_K\ K^2(2J+1)} \Delta V \times\ \tau(J,K)\ Q\ T_{ex}\ exp(E/kT_{rot}),$$

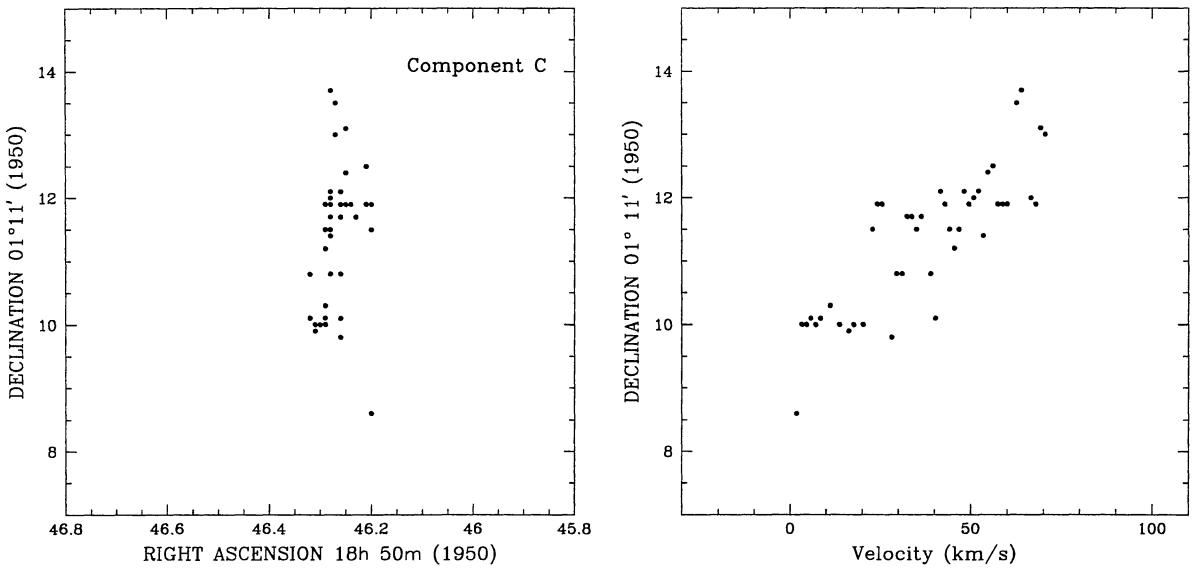

Fig. 5. (Left) Distribution of water maser positions toward component C. (Right) Declination versus radial velocity for the water masers toward component C.

where ν is the transition frequency in GHz, g_K is the statistical weight, E(J,K) is the rotational energy of the (J,K) level above the ground state, ΔV is the line width in km s^{-1}, Q is the partition function, and k is Boltzmann's constant. For $T_{rot} \gg 20$ K, the partition function is given by (e.g., Genzel et al. 1982)

$$Q = 115 \left[\frac{T_{rot}}{200K}\right]^{3/2} .$$

An upper limit to the opacity of the main line of the (3,3) transition, $\tau(3,3;m)$, can be obtained using the expression

$$\frac{S_L(3,3;m)}{S_L(3,3;s)} = \frac{1 - exp[-\tau(3,3;m)]}{1 - exp[-\tau(3,3;m)/33]},$$

where $S(3,3;s)$ is the flux density of a satellite line of the (3,3) transition. For component 4 we estimate, from the spectrum shown in Fig. 4, that $S_L(3,3;m)/S_L(3,3;s) \geq 10$, implying $\tau(3,3;m) \leq 3$. A more direct estimate of $\tau(3,3;m)$ can be derived from the peak brightness temperature, $T_L^b = 3.11(S_L/\Theta_b^2)$, where S_L is in mJy and Θ_b in arcsec. In the (3,3,m) line, clump 4 has a deconvolved angular size of $\sim$8.″1 ($\sim$ 0.15 pc at the distance of 3.8 kpc) and a flux density of $\sim$ 56 $\pm$ 6 mJy. From the radiative transfer equation

$$T_L^b = f(T_{ex} - T_{bg})[1 - exp(-\tau(3,3;m))] \ ,$$

where f is the filling factor, assuming that $T_{ex} = T_{rot} = 54$ K, $T_{bg} = 2.7$ K, and $f = 1$, we find $\tau(3,3;m) \simeq 0.061$. Note that this value provides a lower limit to the (3,3;m) opacity since f is likely to be smaller than 1. Since $\tau(3,3) \simeq 1.12\tau(3,3;m)$, then $\tau(3,3) \simeq 0.068$. The total ammonia column density is $\geq 2.7 \times 10^{15}$ cm^{-2}. Further, the molecular hydrogen density can be estimated from the total column density assuming a path length and a [H_2/NH_3] abundance ratio. For clumps in massive star forming regions a wide range of values of this ratio have been reported, from $\sim 10^6$ to 10^8 (Garay & Lizano 1999; Harju, Walmsley, & Wouterloot 1993). Here we adopt [H_2/NH_3]=10^7. Using a path length of 0.15 pc, equal to the projected linear size, we obtain n(H_2) $\geq 6 \times 10^4$ cm^{-3}. Assuming a spherical structure we then estimate a molecular mass for the clump of $\geq 10\ M_\odot$. An estimate of the virial mass for this clump gives $\sim 300\ M_\odot$. The large difference between the two estimates suggests that the clump is not in virial equilibrium, but probably undergoing expansion and/or outflowing motions. However, given the uncertainties in the mass determination from the ammonia lines, this result is not conclusive.

3.4. *The Molecular Gas around Component C*

As shown in Fig. 3, several of the water maser spots reported by Fey et al. (1994) lay projected between the emission and absorption features seen toward the C component in the (2,2) ammonia line.

In order to investigate if there is any relation between the kinematics of the ammonia gas and the water masers located near the "head" of the H II region we selected all 43 water masers from Fey et al. (1994) in the velocity range from 1.8 to 70.5 km s^{-1}. Masers with velocities higher than this range where not taken into account since it is very unlikely that they could be gravitationally bound. Figure 5 shows the distribution in position and radial velocity of the water masers in the vicinity of the H II region C. To the north the masers are redshifted and to the south they are blueshifted. We measure a velocity shift, ΔV, of $\simeq$ 70 km s^{-1} over an angular extent, $\Delta\Theta$, of $\simeq 5\farcs3$ ($\sim$ 0.098 pc), implying a velocity gradient of $\sim$ 700 km s^{-1} pc^{-1} and a virial mass of $\sim 10^4\ M_\odot$.

The first-order moment slice from the (3,3) ammonia emission through $\alpha(1950) = 18^h\ 50^m\ 46\fs31$ and along a declination from 05″ to 20″ where the water masers appear shows a slight velocity gradient in the same sign as the water masers do, with higher velocities toward the north and lower velocities toward the south. This shift corresponds to a velocity gradient of $\sim$ 15 km s^{-1} pc^{-1}. This value is consistent with other estimates: 13 km s^{-1} pc^{-1} for the $H^{13}CN$, and 20 km s^{-1} pc^{-1} for the SO in 0.2 pc (Carral & Welch 1992); 16 km s^{-1} pc^{-1} for the CH_3CN in 0.18 pc (Akeson & Carlstrom 1996). These values are consistent with a virial mass of $\sim 80 \pm 20\ M_\odot$. We then conclude that the kinematics of the water masers cannot be attributed to bound motions and are most likely the result of shock acceleration.

4. CONCLUSIONS

We found one new warm ammonia clump toward the northwest of the H II region G34.26+0.15. Our study suggests that in addition to the massive stars that excite the H II regions previously reported, there could be other young stars of lower mass in the region. However, the presence of a star embedded in the clump is not certain. On one hand, the association with water masers and the warm temperature of the clump suggest an embedded energy source. On the other hand, the mass of the clump ($\sim 10\ M_\odot$, obtained assuming an $[H_2/NH_3]$ ratio of 10^7) is not very large and the observed temperature ($\sim 54 \pm 12$ K) may be accounted for by heating from the O6 ZAMS star that ionizes the cometary H II region. A comparison of the kinematics of the water masers with the kinematics of the molecular gas at the head of the H II region shows that both have a velocity gradient in the same direction with the blueshifted components to the south and the redshifted to the north. However, the gradient derived from the water masers is nearly two orders of magnitude larger than that derived from other molecular lines suggesting that the kinematics of water masers do not have a gravitationally bound nature.

YG, CR, and LFR acknowledge the support from DGAPA, UNAM, and CONACyT, México. GG acknowledges support from a Chilean Presidential Science Fellowship and Fondecyt Project 1980660. We thank P. Carral for useful discussions.

REFERENCES

Akeson, R. L., & Carlstrom, J. E. 1996, ApJ, 470, 528
Andersson, M., & Garay, G. 1986, A&A, 167, L1
Benson, J., & Johnston, K. 1984, ApJ, 277, 181
Briggs, D. 1995, Ph.D. thesis, New Mexico Institute of Mining and Technology
Carral, P., Kurtz, S., Rodríguez, L. F., Martí, J., Lizano, S., & Osorio, M. 1999, RevMexAA, 35, 97
Carral, P., & Welch, W. J. 1992, ApJ, 385, 244
Carral, P., Welch, W. J., & Wright, M. C. H. 1987, RevMexAA, 14, 506
Churchwell, E., Walmsley, C. M., & Wood, D. O. S. 1992, A&A, 253, 541
Fey, A. L., Claussen, M. J., Gaume, R. A., Nedoluha, G. E., & Johnston, K. J. 1992, AJ, 103, 234
Fey, A. L., Gaume, R. A., Nedoluha, G. E., & Claussen, M. J. 1994, ApJ, 435, 738
Garay, G., & Lizano, S. 1999, PASP, 111, 1049
Garay, G., Reid, M. J., & Moran, J. M. 1985, ApJ, 289, 681
Garay, G., & Rodríguez, L. F. 1990, ApJ, 362, 191
Garay, G., Rodríguez, L. F., & van Gorkom, J. H. 1986, ApJ, 309, 553
Gaume, R. A., Fey, A. L., & Claussen, M. J. 1994, ApJ, 432, 648
Gaume, R. A., & Mutel, R. L. 1987, ApJS, 65, 193
Genzel, R., & Downes, D. 1977, A&AS, 30, 145
Genzel, R., Ho, P. T. P., Bieging, J., & Downes, D. 1982, ApJ, 259, L103
Harju, J., Walmsley, C. M., & Wouterloot, J. G. A. 1993, A&AS, 98, 51
Heaton, B. D., Little, L. T, & Bishop, I. S. 1989, A&A, 213, 148
Heaton, B. D., Little, L. T, Yamashita, T., Davies, S. R., Cunningham, C. T., & Monteiro, T. S. 1993, A&A, 278, 238
Heaton, B. D., Matthews, N., Little, L. T., & Dent, W. R. F. 1985, MNRAS, 217, 485
Henkel, C., Wilson, T. L., & Mauersberger, R. 1987, A&A, 182, 137
Hunter, T. R., Neugebauer, G., Benford, D. J., Matthews, K., Lis, D. C., Serabyn, E., & Phillips, T. G. 1998, ApJ, 493, L97
Keto, E., Ho, P. T. P., & Reid, M. J. 1987, ApJ, 323, 117

Natta, A., Palla, F., Preite-Martinez, A., & Panagia, N. 1981, A&A, 99, 289
Reid, M. J., & Ho, P. T. P. 1985, ApJ, 288, L17
Ryle, M., & Downes, D. 1967, ApJ, 148. L17
Turner, B. E., Balick, B., Cudaback, D. D., Heiles, C., & Boyle, R. J. 1974, ApJ, 194, 279
Schwab, F. 1980, Proc. SPIE, 231, 18
Scoville, N. Z., & Kwan, J. 1976, ApJ, 206, 718
Watt, S., & Mundy, L. G. 1999, ApJS, 125, 143
Wood, D. O. S., & Churchwell, E. 1989, ApJS, 69, 835

Yolanda Gómez, Carlos A. Rodríguez-Rico, and Luis F. Rodríguez: Instituto de Astronomía, UNAM, Campus Morelia, Apartado Postal 3-72 (Xangari), 58089 Morelia, Michoacán, México (gocy,carlos,luisfr@astrosmo.unam.mx).
Guido Garay: Departamento de Astronomía, Universidad de Chile, Casilla 36-D, Santiago, Chile (guido@das.uchile.cl).